Molecular BioSystems

PAPER

View Article Online
View Journal | View Issue

Cite this: *Mol. BioSyst.*, 2014, **10**, 1332

Mitochondrial proteomics investigation of a cellular model of impaired dopamine homeostasis, an early step in Parkinson's disease pathogenesis†

Tiziana Alberio,[ab] Heather Bondi,[ab] Flavia Colombo,[a] Isabella Alloggio,[cd] Luisa Pieroni,[de] Andrea Urbani*[de] and Mauro Fasano*[ab]

Received 23rd December 2013,
Accepted 10th March 2014

DOI: 10.1039/c3mb70611g

www.rsc.org/molecularbiosystems

Impaired dopamine homeostasis is an early event in the pathogenesis of Parkinson's disease. Generation of intracellular reactive oxygen species consequent to dopamine oxidation leads to mitochondrial dysfunction and eventually cell death. Alterations in the mitochondrial proteome due to dopamine exposure were investigated in the SH-SY5Y human neuroblastoma cell line. The combination of two orthogonal proteomic approaches, two-dimensional electrophoresis and shotgun proteomics (proteomeXchange dataset PXD000838), was used to highlight the specific pathways perturbed by the increase of intracellular dopamine, in comparison with those perturbed by a specific mitochondrial toxin (4-methylphenylpyridinium, MPP^+), a neurotoxin causing Parkinsonism-like symptoms in animal models. Proteins altered by MPP^+ did not completely overlap with those affected by dopamine treatment. In particular, the MPP^+ target complex I component NADH dehydrogenase [ubiquinone] iron–sulfur protein 3 was not affected by dopamine together with 26 other proteins. The comparison of proteomics approaches highlighted the fragmentation of some mitochondrial proteins, suggesting an alteration of the mitochondrial protease activity. Pathway and disease association analysis of the proteins affected by dopamine revealed the overrepresentation of the Parkinson's disease and the parkin–ubiquitin proteasomal system pathways and of gene ontologies associated with generation of precursor metabolites and energy, response to topologically incorrect proteins and programmed cell death. These alterations may be globally interpreted in part as the result of a direct effect of dopamine on mitochondria (*e.g.* alteration of the mitochondrial protease activity) and in part as the effect on mitochondria of a general activation of cellular processes (*e.g.* regulation of programmed cell death).

Introduction

Parkinson's disease is a complex multifactorial movement disorder associated with a spectrum of distinct pathologies.[1] Useful insights have been gained, thanks to cellular and animal models of PD pathogenesis.[2,3] Several pathogenetic factors lead to mitochondrial impairment that eventually determines selective degeneration of nigrostriatal dopaminergic neurons. Impaired dopamine homeostasis appears to be a key factor in the early steps to PD pathogenesis.[2–5] Dopamine shows a marked propensity to auto-oxidation, with the concurrent generation of reactive oxygen species (ROS) and dopamine quinone (DAQ). These chemicals induce mitochondrial impairment by activating the intrinsic apoptosis pathway (ROS) or by inhibiting the respiratory chain (DAQ).[4,5] Dopamine homeostasis might be altered by pre-fibrillar intermediates of α-synuclein, a protein earlier linked to familial PD, which associates with vesicles and induces dopamine leakage.[1,4] Also the impairment of protein clearance, either by the ubiquitin-proteasome system (UPS) or by autophagy, contributes to neural loss in PD.[6,7] The identification of parkin as an ubiquitin E3 ligase, together with the reported mutations of the deubiquitinating enzyme UCH-L1 in rare cases of a single PD family, has suggested that a failure in the UPS might significantly contribute to PD pathogenesis.[8]

Many pieces of evidence suggest that mitochondrial dysfunction in post-mitotic cells such as neurons can lead to cell death.[9] Alterations in the oxidative phosphorylation have been associated with the pathogenesis of neurodegenerative disorders.[10,11]

[a] *Biomedical Research Division, Department of Theoretical and Applied Sciences, University of Insubria, Busto Arsizio, Italy. E-mail: mauro.fasano@uninsubria.it; Fax: +39 0332 395599; Tel: +39 0331 339450*
[b] *Center of Neuroscience, University of Insubria, Busto Arsizio, Italy*
[c] *DIVET, Department of Veterinary Science and Public Health, University of Milan, Milan, Italy*
[d] *Santa Lucia IRCCS Foundation, Rome, Italy*
[e] *Department of Experimental Medicine and Surgery, University of Rome "Tor Vergata", Rome, Italy. E-mail: andrea.urbani@uniroma2.it; Fax: +39 06 50170 3332; Tel: +39 06 50170 3215*

† Electronic supplementary information (ESI) available: Tables S1–S4, Fig. S1–S5. See DOI: 10.1039/c3mb70611g

Toxins such as MPP^+ and rotenone are capable of damaging dopaminergic cells because they are taken up through the dopamine transporter (DAT) and block the mitochondrial respiratory chain, with the consequent activation of apoptotic cell death.[2,12] The functionality of the respiratory chain is also maintained by the turnover of mitochondrial complexes selectively mediated by the PINK1/parkin pathway through a mechanism that is independent by the classic autophagy activation.[13] However, the role played by mitochondrial dysfunction in the PD pathogenesis is not limited to the respiratory chain failure, but also involves their dynamics, with consequent modifications of their morphology, trafficking and quality control.[11,14]

Mitochondrial dysfunction and autophagy are strictly connected. Indeed, damaged mitochondria are removed through macroautophagy (mitophagy), in order to reduce the activation of apoptosis. If this clearance process is impaired, an enhancement of oxidative stress is expected to occur.[2,15] Proteins associated with autosomal-recessive PD have been linked to mitophagy. Parkin translocates to mitochondria upon dissipation of the mitochondrial membrane potential ($\Delta\Psi_m$) by the uncoupler carbonyl cyanide *m*-chlorophenylhydrazone (CCCP) or in response to ROS.[16] As a result, damaged mitochondria are removed by mitophagy. Functional PINK1, a mitochondrial serine-threonine kinase that affords protection against oxidative stress, is a prerequisite to induce translocation of the E3 ligase parkin to depolarized mitochondria.[17] These data provide therefore functional links between PINK1, parkin and selective autophagy of mitochondria.[18]

In the present study, we investigate the effect of dopamine on the expression pattern of mitochondrial proteins in the undifferentiated human catecholaminergic neuroblastoma cell line SH-SY5Y, a widely used cellular model that reproduces impaired dopamine homeostasis, which is a possible pivotal aspect in the pathogenesis of PD.[2] These cells possess a complete dopaminergic system. In particular, they couple the good activity of the dopamine transporter (DAT) with the low activity of the vesicular monoamine transporter type 2, so that the cytoplasmic dopamine concentration may be raised by administration of exogenous dopamine in the culture medium.[2,19] As a reference, MPP^+ is used to induce mitochondrial impairment through specific complex I inhibition. In this context, the proteomic identification of mitochondrial proteins altered by disruption of dopamine homeostasis may significantly help to understand alterations of mitochondrial functionality in PD pathogenesis.

Furthermore, these findings will contribute to the worldwide project promoted by the Human Proteome Organization (HUPO) both at the chromosome-centric and biological-disease levels,[20] within which the Italian Proteomics Association (ItPA) has initiated the mitochondrial Human Proteome Project (mt-HPP).[21]

Results

Cytotoxicity assays

The toxic effect of dopamine and MPP^+ on SH-SY5Y cells was evaluated by observing the relative cell viability after exposure to the toxic insult. Fig. 1 reports the dose dependent toxicity of dopamine (panel A) and MPP^+ (panel B). Dopamine significantly affected cell viability at 250 μM concentration, with a decrease of about 40%. Therefore, this concentration was selected for further experiments. The MPP^+ concentration used (2.5 mM) was chosen in order to have a significant viability reduction similar to that observed for dopamine.

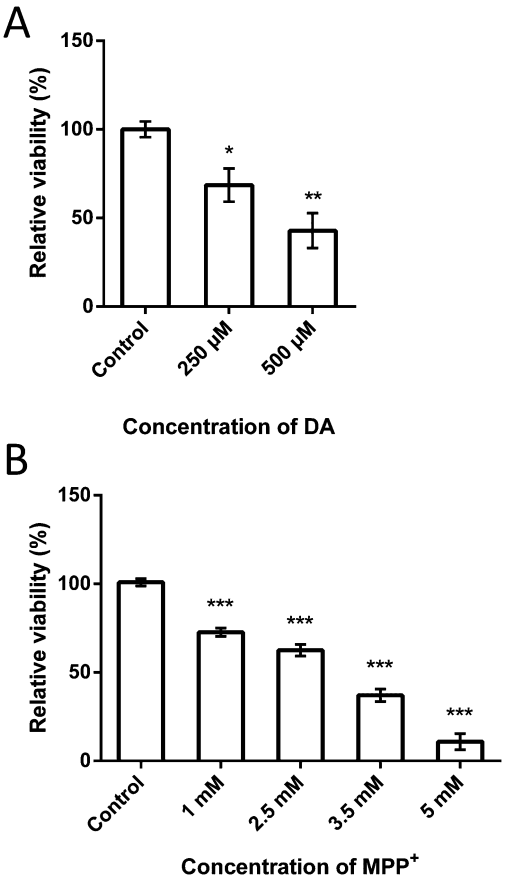

Fig. 1 Cell viability of SH-SY5Y cells. (A) relative cell viability in the absence and in the presence of 250 and 500 μM dopamine. (B) relative cell viability in the absence and in the presence of 1.0 to 5.0 mM MPP^+. *$p < 0.05$; **$p < 0.01$; ***$p < 0.005$.

Mitochondrial fraction enrichment

Effectiveness of the mitochondrial enrichment procedure was evaluated by western blotting. Fig. 2, panel A shows that the mitochondrial marker VDAC1 was noticeably enriched in the mitochondrial fraction and almost undetectable in the cytosolic fraction. The nuclear marker histone H3, which was very abundant in the unfractionated sample, was fairly detectable in its full-length form in the cytosolic fraction and in its processed form in the mitochondrial fraction, thus indicating a mild co-enrichment of nuclei in the latter sample. On the other hand, a more consistent presence of the cytosolic marker β-actin might be appreciated, thus suggesting a remarkable enrichment of cytosolic proteins that interact with mitochondria, such as β-actin.

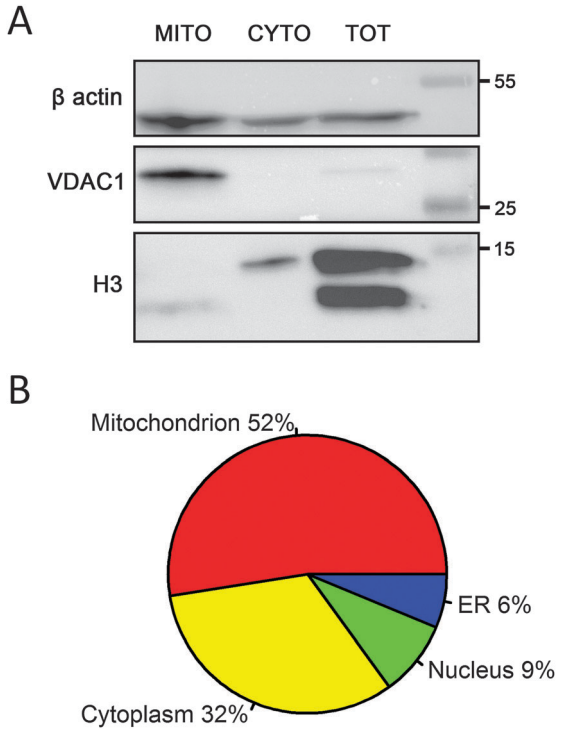

Fig. 2 Mitochondria enrichment. Panel A: a representative western blot of cytoplasmic (β-actin), mitochondrial (VDAC1) and nuclear (H3) markers of mitochondrial, cytosolic and total fractions. Panel B: distribution of Gene Ontology cell component classification for proteins identified by Shotgun proteomics.

Functional classification of proteins observed in shotgun proteomics experiments (see below) also indicated a substantial higher number of proteins identified as mitochondrial according to the DAVID gene ontology classification engine (Fig. 2, panel B). Among the most abundant proteins, 52% were mitochondrial proteins, 9% were nuclear and only 6% from the endoplasmic reticulum (ER). A more consistent fraction of enriched proteins was composed of cytoskeletal or cytoskeleton-associated proteins. Eventually, the recurrent presence of mitochondrial matrix proteins in the Shotgun identification might ensure that no significant damage occurred in mitochondria isolation.

Shotgun proteomics of mitochondrial fractions

To perform a differential analysis of the protein repertoire in the mitochondrial fractions, an experiment of Label Free Differential Proteomics by Data Independent Analysis was designed based on a Shotgun discovery proteomics methodology. This approach is taking advantage of the high reproducibility of retention time elution profiles given the employment of a nano-Ultra Performance Liquid Chromatography (nUPLC) system. In particular, the experiments were performed by means of nUPLC coupled to a high/low collision energy MS (MS^E)-based label free quantitative shotgun approach, *i.e.*, a Waters nanoAcquity UPLC System coupled to a Waters Q-TOF Premiere tandem mass spectrometer. Since there was no isotopic labeling of the samples, data complexity was reduced and the mass spectrometry analysis provided a deeper view in the repertoire of less abundant proteins. Such a feature made this approach thoroughly applied in the proteomics community in order to collect wide MS-based datasets.[22]

To take into account the variability due to the experimental procedure, the mitochondrial fractions from SH-SY5Y treated with DA or MPP^+ were compared to control samples (control) by including all technical and biological replicates in a single group, *i.e.*, four technical LC-MS^E runs for each of the three biological replicates of the same condition. Quality assessment of the data was evaluated by the analytical performances on the actual experimental dataset (Fig. S1 in the ESI†). The average distribution of the coefficient of variation (CV%) of peptide signal intensity was around 2.5%, while the CV% of retention times was centered on 1.5%. However, to keep a conservative approach protein hits were filtered to a fold difference larger than 30%. These performances are in line with those previously reported.[23–27]

To achieve a greater level of confidence, two independent procedures of comparative statistics analysis were performed. The first one was based on the proprietary build-in expression analysis embedded in the PLGS software. The second one was based on a parametric (paired *t*-test) comparison of protein amount values as obtained from the protein identity procedure (Fig. S2 in the ESI;† see the Experimental section for further details). Table 1 reports all protein identities that showed significant variation in at least one contrast (*i.e.*, DA *vs.* control, MPP^+ *vs.* control, MPP^+ *vs.* DA).

Mitochondrial protein expression analysis by two-dimensional electrophoresis

Mitochondrial fractions were analyzed by 2-DE with fluorescent staining (Fig. 3). Spots were automatically detected and extensively refined to filter out any error in the detection and matching procedures. A total of 652 spots were assigned to each group (control group; DA, dopamine treatment group; MPP, MPP^+ treatment group). Among them, 220 had two or more missing values in each group and were removed. A subset of 136 spots present in all 15 gels was used for relative normalization. The quality of the gels was checked by pairwise comparisons and residuals of each linear fitting were compared in a normal distribution *vs.* a ranked distribution (Quantile–Quantile plots; Fig. S3 in the ESI†). The worst performing gel in each group was excluded from the further analysis. Residual missing values were replaced as described in the experimental procedures.

Normalized spot volumes were analyzed by the non-parametric Kruskal–Wallis test to identify which were significantly associated with at least one group, followed by the *post hoc* Dunn's test to identify which contrast was responsible for the observed significance (see Fig. S4 in the ESI†). In this way, 23 spots were excised for protein identification by ESI-TRAP LC/MS (see Table S1 in the ESI†). Table 2 summarizes 2-DE image analysis results with protein identification. In case of multiple identifications for a single 2-DE spot, the protein with measured pI and MW values more consistent with theoretical ones was chosen. Nevertheless, each protein assignment was supported by an extensive literature analysis, as well as database search.

Table 1 Summary of identification of differentially expressed proteins by shotgun proteomics

UniProt ID	Protein name	PLGS score	Observed change	Fold of change (log_2)[c]	Subcellular localization
A5A3E0[a]	POTE ankyrin domain family member F	7077.73	↑DA	0.77	Cytoplasm
O75390[b]	Citrate synthase	n.a.	↑DA		Mitochondrion
			↓MPP^+		
P02545[a]	Prelamin-A/C	113.7	↓MPP^+[d]	−0.60	Nucleus
P04075[a,b]	Fructose-bisphosphate aldolase A	112.51	↑DA	1.63	Cytoplasm
P04406[a,b]	Glyceraldehyde-3-phosphate dehydrogenase	3279.28	↑DA	0.43	Cytoplasm
			↑MPP^+	0.63	
P05141[a]	ADP/ATP translocase 2	1672.64	↑DA	1.63	Mitochondrion
			↑MPP^+	1.85	
P07339[b]	Cathepsin D	n.a.	↑DA		Mitochondrion
P07355[a,b]	Annexin A2	577.69	↑MPP^+[d]	0.46	Cytoplasm
P07437[a]	Tubulin beta chain	999.93	↓DA	−0.36	Cytoplasm
P08107[a]	Heat shock 70 kDa protein 1A/1B	884.91	↑DA	0.75	Cytoplasm
			↑MPP^+	0.70	
P08238[a]	Heat shock protein HSP 90-beta	565.32	↑DA	0.25	Mitochondrion
			↑MPP^+	0.43	
P08670[a,b]	Vimentin	312.14	↓MPP^+[d]	−0.94	Cytoplasm
P08865[a]	40S ribosomal protein SA	168.34	↑DA	0.72	Cytoplasm
			↓MPP^+	−0.17	
P10809[b]	60 kDa heat shock protein	n.a.	↑MPP^+		Mitochondrion
P0CG38[a]	POTE ankyrin domain family member I	4804.99	↓DA	−0.40	Cytoplasm
			↑MPP^+	0.32	
P11021[a,b]	78 kDa glucose-regulated protein	567.39	↑DA	0.62	Endoplasmic reticulum
			↑MPP^+	0.70	
P12236[a]	ADP/ATP translocase 3	1964.34	↑DA	0.85	Mitochondrion
			↑MPP^+	0.85	
P14618[a,b]	Pyruvate kinase PKM	937.49	↑DA	1.49	Cytoplasm
P14625[a]	Endoplasmin	73.66	↑DA	0.51	Endoplasmic reticulum
			↑MPP^+	0.85	
P16401[a,b]	Histone H1.5	839.56	↑DA	0.65	Nucleus
			↑MPP^+	0.99	
P17066[a]	Heat shock 70 kDa protein 6	873.17	↑DA	0.86	Cytoplasm
			↑MPP^+	0.52	
P21796[a,b]	Voltage-dependent anion-selective channel protein 1	2259.26	↑DA	0.39	Mitochondrion
			↑MPP^+	0.49	
P23528[a]	Cofilin-1	9265.04	↑DA	1.26	Cytoplasm
			↓MPP^+	−0.30	
P29966[a,b]	Myristoylated alanine-rich C-kinase substrate	1457.41	↑DA[a]	0.46	Cytoplasm
			↑MPP^+[b]		
P30048[b]	Peroxiredoxin-3	n.a.	↑DA		Mitochondrion
			↑MPP^+		
P30101[a,b]	Protein disulfide-isomerase A3	326.33	↑MPP^+[d]	0.54	Endoplasmic reticulum
P34897[b]	Serine hydroxymethyltransferase	n.a.	↑DA		Mitochondrion
P34931[a]	Heat shock 70 kDa protein 1-like	1289.22	↑MPP^+	0.59	Mitochondrion
P35232[a,b]	Prohibitin	3478.43	↑DA	0.30	Mitochondrion
			↑MPP^+	0.54	
P38646[b]	Mortalin	n.a.	↑MPP^+		Mitochondrion
P40926[b]	Malate dehydrogenase	n.a.	↑MPP^+		Mitochondrion
P42704[b]	Leucine-rich PPR motif-containing protein	n.a.	↑MPP^+		Mitochondrion
P45880[a,b]	Voltage-dependent anion-selective channel protein 2	2218.59	↑DA	0.30	Mitochondrion
			↑MPP^+	0.58	
P49411[a,b]	Elongation factor Tu	4284.08	↑DA[b]	−1.09	Mitochondrion
			↓MPP^+[a,b]		
P60709[a]	Beta-actin	16 414.67	↓DA	−0.54	Cytoplasm
			↓MPP^+	−0.86	
P62805[a,b]	Histone H4	22 497.28	↑DA	0.30	Nucleus
			↑MPP^+	1.52	
P62807[a]	Histone H2B	4979.12	↑MPP^+	1.55	Nucleus
P62937[b]	Cyclophilin A	n.a.	↑MPP^+		Cytoplasm
P62987[a]	Ubiquitin-60S ribosomal protein L40	5678.05	↑MPP^+	0.42	Cytoplasm
P68104[a,b]	Elongation factor 1-alpha 1	3410.02	↑DA	1.55	Cytoplasm
			↑MPP^+	0.96	
P68363[a]	Tubulin alpha-1B chain	4027.61	↑MPP^+	0.63	Cytoplasm
Q00325[a,b]	Phosphate carrier protein	665.66	↑MPP^+	0.85	Mitochondrion
Q07021[b]	Complement component 1 Q subcomponent-binding protein	n.a.	↑DA		Mitochondrion
			↑MPP^+		
Q16181[b]	Septin-7	n.a.	↑MPP^+		Nucleus
Q16695[a]	Histone H3	5573.15	↑MPP^+	1.80	Nucleus
Q16891[b]	Mitofilin	n.a.	↑MPP^+		Mitochondrion

Table 1 (*continued*)

UniProt ID	Protein name	PLGS score	Observed change	Fold of change ($\log_2$)[c]	Subcellular localization
Q562R1[a]	Beta-actin-like protein 2	2637.17	↓DA ↓MPP^+	−0.47 −0.49	Cytoplasm
Q58FF8[a]	Heat shock protein 90-beta b	n.a.	Control only	n.a.	Cytoplasm
Q6S8J3[a]	POTE ankyrin domain family member E	5043.7	↓MPP^+[d]	−1.74	Cytoplasm
Q71UI9[a]	Histone H2A	2814.1	↑MPP^+[d]	0.68	Nucleus
Q8IV08[a,b]	Phospholipase D3	209.38	↑DA[a,b] ↓MPP^+[b]	1.77	Endoplasmic reticulum
Q99623[a,b]	Prohibitin-2	1594.88	↑MPP^+	0.58	Mitochondrion
Q9BQE3[a]	Tubulin alpha-1C chain	1689.2	↓MPP^+[d]	−0.74	Cytoplasm
Q9BYX7[a]	POTE ankyrin domain family member K	6232.57	↑DA	1.26	Cytoplasm
Q9H9B4[a,b]	Sideroflexin-1	265.92	↑MPP^+	0.46	Mitochondrion
Q9UJS0[a,b]	Calcium-binding mitochondrial carrier protein Aralar2	543.43	↑MPP^+	0.48	Mitochondrion
Q9Y277[b]	Voltage-dependent anion-selective channel protein 3	n.a.	↑MPP^+		Mitochondrion

n.a.: not applicable. [a] Quantitative expression analysis. [b] Semi-quantitative analysis of amount values from protein identity tables. [c] The fold of change is reported for the quantitative expression analysis only. [d] With respect to DA.

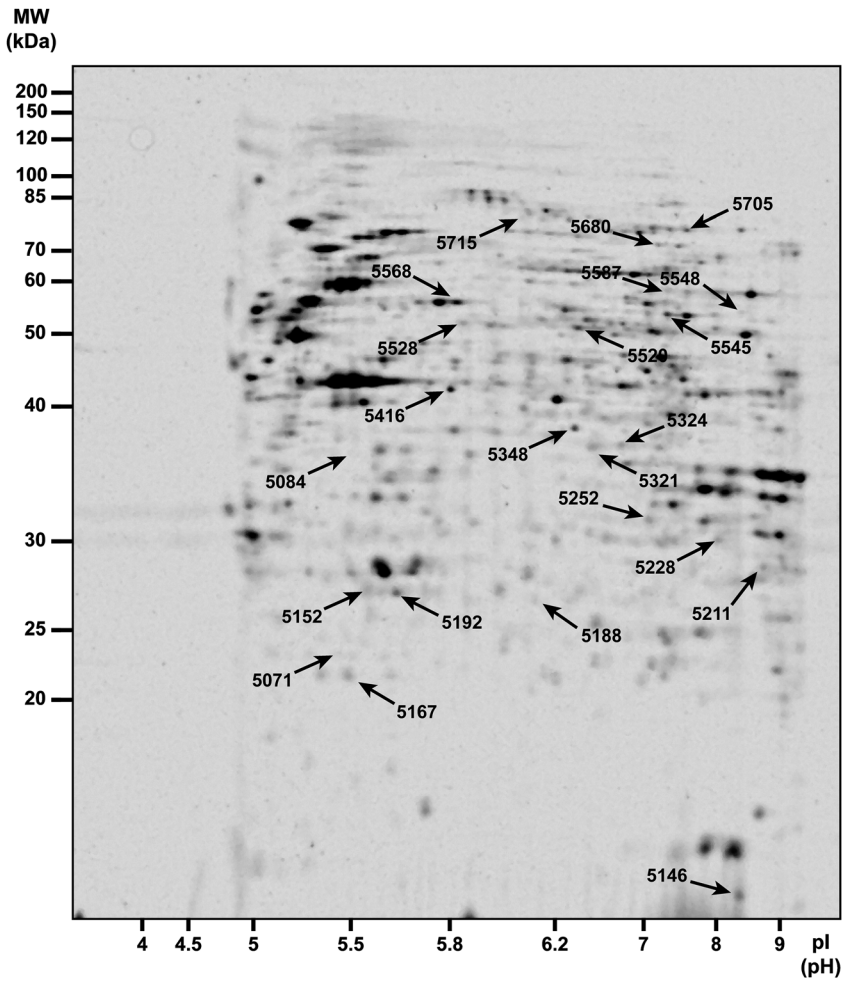

Fig. 3 A representative 2-DE image of mitochondrial fractions from SH-SY5Y cells. Spots that were identified to be significantly associated with an experimental group are labeled.

Bioinformatics analysis

The list of proteins that showed altered levels after dopamine treatment (Table S2 in the ESI†), independently by the MPP^+ effect, was used to perform the enrichment analysis and interpret the results obtained by the two proteomic approaches.

First of all, different tools of Webgestalt were exploited to obtain biological insights from the list. The Gene Ontology

Table 2 Summary of 2-DE image analysis with protein identification

Spot ID	Identified proteins	UniProt AC	Mascot score	Protein sequence coverage (%)	Theoretical MW (kDa)/pI	Measured MW (kDA)/pI	Observed change	Fold of change (log_2 units)	P value[a]
5084	Actin	P60709	699	40.5	42/5.3	39/5.5	↑DA	1.6	0.047
5146	Single-stranded DNA-binding protein	Q04837	381	59.5	13/9.5	10/8.5	↑DA	0.9	0.023
							↑MPP^+	1.0	
5152	Prohibitin	P35232	74	17.3	30/5.6	26/5.6	↑DA[b]	0.7	0.033
							↓MPP^+	−1.2	
5167	ATP synthase subunit d	O75947	167	39.8	18/5.2	19/5.5	↑DA[b]	0.9	0.013
							↓MPP^+	−0.4	
5188	Mortalin	P38646	38	11.6	74/5.9	25/5.6	↑DA	1.5	0.027
5192	NADH dehydrogenase [ubiquinone] iron–sulfur protein 3	O75489	410	33.7	26/5.5	25/5.6	↓MPP^+	−1.4	0.008
5211	ATP synthase subunit alpha	P25705	42	15	55/8.3	27/8.5	↑MPP^+	1.9	0.019
5228	Guanine nucleotide-binding protein subunit beta-2-like 1	P63244	245	47.3	35/7.6	30/8.0	↑DA	1.2	0.017
5252	Voltage-dependent anion-selective channel protein 2	P45880	46	7.5	32/7.5	32/7.2	↓DA	−1.4	0.027
5321	Phospholipase D3	Q8IV08	57	2	55/6.0	40/6.4	↓DA	−1.4	0.007
	Pyruvate kinase isozymes M1/M2	P14618	64	14.3	58/8.0		↓MPP^+	−1.7	
5324	Elongation factor Tu	P49411	40	13.7	45/6.3	40/6.5	↓MPP^+	−1.3	0.009
5348	Annexin A3	P12429	158	21.7	37/5.6	42/8.4	↑DA[b]	1.5	0.039
							↓MPP^+	−2.0	
5416	Prelamin-A/C	P02545	587	34.8	72/6.4	48/5.8	↑DA[b]	0.8	0.042
	Actin	P60709	123	30.1	42/5.3		↓MPP^+	−0.7	
5520	RuvB-like 1	Q9Y265	371	40.1	50/6.0	58/6.3	↑DA	1.7	0.004
	Phospholipase D3	Q8IV08	116	8.4	55/6.0				
5528	Not identified	N/A	N/A	N/A	N/A	58/5.8	↑DA[b]	0.1	0.023
							↓MPP^+	−0.8	
5545	Pyruvate kinase isozymes M1/M2	P14618	282	27.3	58/8.0	60/7.5	↓MPP^+	−1.4	0.023
5548	Adenylyl cyclase-associated protein 1	Q01518	49	14.1	52/8.3	61/8.5	↑MPP^+	1.2	0.015
5568	Protein disulfide-isomerase A3	P30101	114	25.3	54/5.6	62/5.8	↓DA	−1.1	0.016
5587	Pyruvate kinase isozymes M1/M2	P14618	38	20.8	58/8.0	65/7.3	↑DA	1.2	0.006
	Helicase SRCAP	Q6ZRS2	37	2.5	343/5.7		↑MPP^+	1.3	
5680	Far upstream element-binding protein 1	Q96AE4	52	19.9	67/7.3	75/7.2	↑MPP^+	0.7	0.042
5705	Septin-9	Q9UHD8	83	20.1	65/9.1	78/7.7	↓DA	−1.0	0.024
5715	Nucleolin	P19338	114	9.2	77/4.6	81/6.1	↑DA	2.1	0.009
							↑MPP^+	1.7	

[a] Kruskal–Wallis test. [b] Distributions are different between DA and MPP^+ after Dunn's *post hoc* test.

enrichment analysis revealed the three major biological processes involved in the response to dopamine treatment: the generation of precursor metabolites and energy (GO:0006091; adjP = 4.6×10^{-3}), the response to topologically incorrect proteins (GO:0035966; adjP = 4.6×10^{-3}) and the programmed cell death (GO:0012501; adjP = 5.8×10^{-3}). Since samples were enriched in mitochondria, these organelles are overrepresented in the GO Cellular Component enrichment, as expected. Interestingly, proteins of mitochondrial nucleoids (GO:0042645; adjP = 1.41×10^{-8}), involved in mtDNA replication and transcription, appeared to be specifically altered by dopamine.

The KEGG pathway enrichment analysis allowed us to highlight the presence of five proteins (Voltage Dependent Anion Channel 1 and 2, ADP/ATP translocase 2 and 3, ATP synthase subunit d) associated with the Parkinson's disease pathway (KEGG pathway 05012; adjP = 4.11×10^{-6}), while the Wikipathway analysis stressed the importance of HSP70 in the Parkin–Ubiquitin Proteasomal System pathway (PW:0000144; adjP = 2.0×10^{-4}).

The disease association analysis (Table S3 in the ESI†) revealed a specific association of several proteins altered by dopamine with the aspecific events ''shock'' (DB_ID:PA445644) and ''stress'' (DB_ID:PA445752), but also with the specific category ''mitochondrial diseases'' (DB_ID:PA447172).

The list of proteins altered by dopamine treatment was also analyzed by Bioprofiling. Fig. 4 shows a significant ($p < 0.005$) network model generated by the PPI spider tool that considers physical interactions reported in the IntAct database. The enrichment might reveal other possible actors of response to dopamine that were not detected by the proteomic analysis. Thirty-five experimentally identified proteins were included in a single model, where no more than one enriched protein was added to connect them. Database evidence for each interaction is reported in Table S4 in the ESI.† Proteins related to cellular component movement, regulation of NF-κB cascade, glycolysis, chromatin modifications, response to unfolded proteins, response to stress, apoptosis, protein folding, nucleosome assembly and DNA replication were found to be significantly enriched.

Discussion

Impaired dopamine homeostasis affects mitochondrial functionality at various levels.[28] Here, the effect of dopamine on the proteome of mitochondria-enriched fractions was evaluated by using two complementary, orthogonal proteomics approaches, at the protein and peptide levels.[25] Mitochondria were obtained

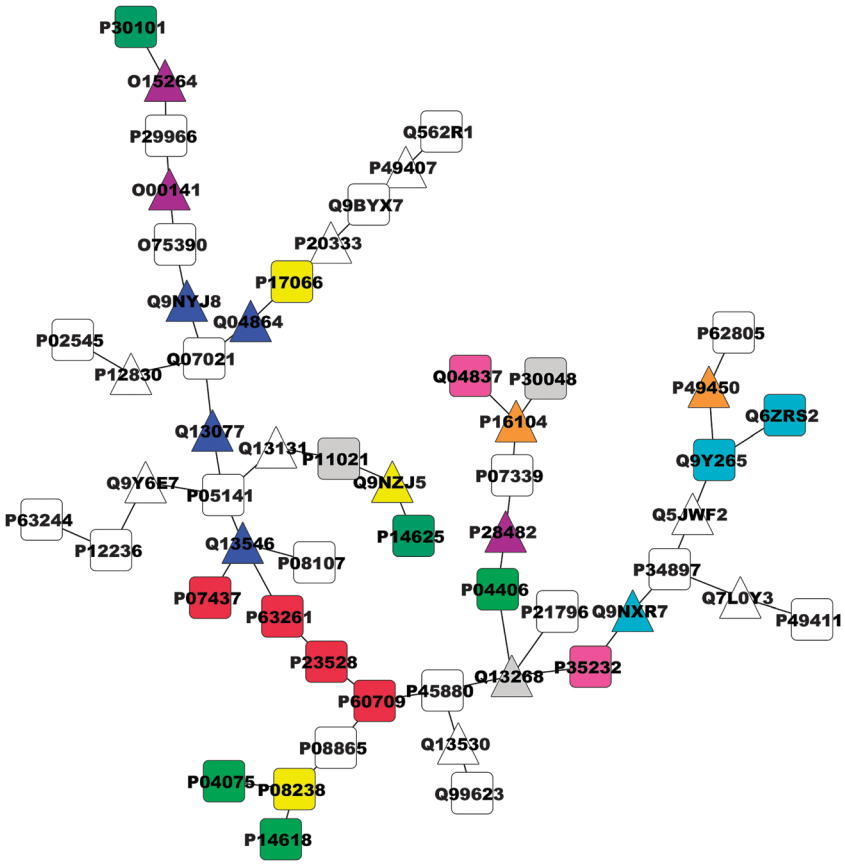

Fig. 4 Enriched network analysis of proteins altered by the dopamine treatment. The network model covers 55 proteins inferred from 47 differentially expressed proteins (35 were mapped to the PPI network). Proteins from the input list are represented by squares. Intermediate genes added by the enrichment tool are represented by triangles. Colors indicate gene functional role according to the Gene Ontology: red, cellular component movement; blue, regulation of NF-κB cascade; light green, glycolysis; cyan, chromatin modifications; yellow, response to unfolded proteins; purple, response to stress; gray, apoptosis; dark green, protein folding; orange, nucleosome assembly; magenta, DNA replication.

from a well established cellular model of dopamine homeostasis impairment, the undifferentiated human neuroblastoma SH-SY5Y cell line treated or not with dopamine in the presence of the extracellular peroxide scavenger catalase.[2,19,29,30]

Although subcellular proteomes are obtained with the purpose of simplifying the complexity of the biological specimen under study, mitochondria-enriched fractions are usually difficult to be investigated with gel-based techniques.[31] Indeed, the heterogeneous distribution of mitochondrial proteins in terms of hydrophobicity, molecular weight and pI, together with the high lipid and nucleic acid contents of mitochondria, prevent a correct focusing. Moreover, the fine-tuning of the cell homogenation conditions, including the composition of the cell lysis buffer, is an essential step to avoid incomplete extraction of hydrophobic proteins, unpredictable leakage of matrix proteins or co-isolation of other organelles such as nuclei or ER.[31,32] Therefore, all the conditions to obtain reproducible 2-DE maps starting from cultured cells were revisited and optimized.

The Shotgun proteomics approach may represent a useful strategy to address all the technical difficulties associated with mitochondria-enriched fractions. Based on gel-free chromatographic separation, it shows better sensitivity and resolution than 2-DE, thus allowing the detection and quantification of several hundreds of proteins. However, as a consequence of the robustness of the experimental design aimed at avoiding type-I (alpha) errors in the selection of significant features,[33] a narrow number of proteins was reported to change. As far as 2-DE is concerned, it provides a better workbench for the characterization of post-translational modifications, including proteolytic degradation.[34] Hence, enriched fractions were analyzed with both peptide- and protein-based approaches, with a remarkable overlapping of the proteins affected by any treatment (Fig. 5A). Proteins that were observed to change in the same way with both techniques are intrinsically validated, whereas proteins that were identified by a single technique might complement the description of the biochemical pathways being involved. Additionally, Shotgun proteomics provides information on protein total levels, whereas 2-DE may account for protein modifications and cleavage. On the other hand, proteins targeted by MPP^+ did not completely overlap with those altered by dopamine treatment (Fig. 5B). Among the latter, only eight proteins were specifically regulated or modified by DA. Conversely, 27 proteins were exclusively altered by MPP^+, which included the MPP^+ target complex I component NADH dehydrogenase [ubiquinone]

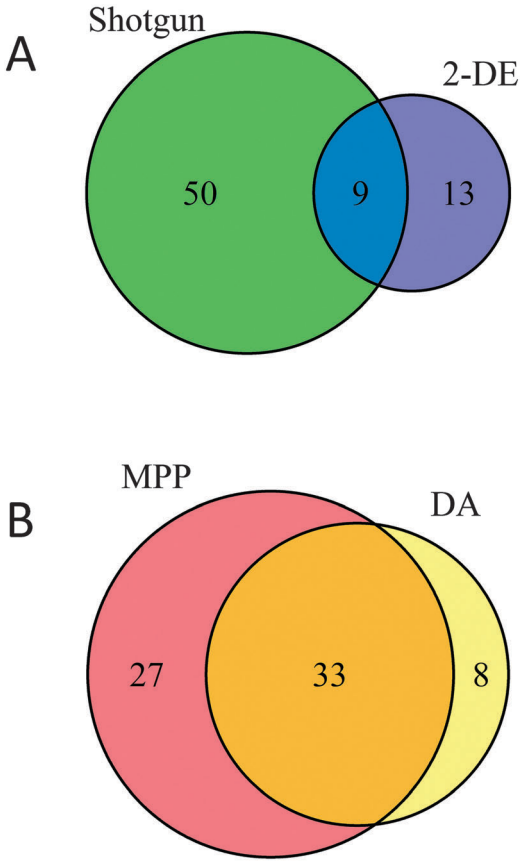

Fig. 5 Euler–Venn diagrams. Panel A: distribution of proteins observed to change using the two experimental techniques. Panel B: distribution of proteins observed to change by treatment.

iron–sulfur protein 3.[35] This suggests that the broad spectrum of modifications induced by dopamine does not completely include the changes evoked by specifically blocking complex I activity.

The combination of orthogonal proteomic approaches may also lead to discrepancies that deserve further investigation. This is the case of the voltage-dependent anion channel isoform 2 (VDAC2). Although this protein appeared to be upregulated in the Shotgun analysis by both treatments (+0.30 and +0.58 fold in $\log_2$ scale by dopamine and MPP^+, respectively), 2-DE analysis highlighted a significant reduction (−1.4-fold in $\log_2$ scale) of the spot identified as VDAC2 after DA exposure. It should be noticed, however, that the VDAC2 band at 32 kDa almost disappeared after dopamine treatment (western blot, see Fig. S5 in the ESI†). Therefore, the present finding might indicate the accumulation of proteolytic peptides within mitochondria, thus suggesting the activation of mitochondrial proteases such as the intermembrane space protease HTRA2/OMI.[36,37] Interestingly, HTRA2 was associated with a familial Parkinsonism (PARK13), although mutations were also found in healthy subjects.[8]

The different activity of mitochondrial proteases with respect to the treatments could also explain the complex behavior displayed by the mitochondrial chaperone mortalin. Indeed, MPP^+ led to a significant increase of mortalin total level, probably in response to cellular stress induced by direct complex I inhibition, but no changes were observed after DA exposure. Interestingly, the level of a mortalin proteolytic 25 kDa fragment, also reported in the Swiss-2DPAGE database (map = LIVER_HUMAN, ac = P38646), was found to be increased only after DA treatment (1.5-fold in $\log_2$ scale). It is noteworthy that mortalin is reduced in nigral neurons of PD patients as found out by proteomics investigations.[38] Even the scaffold proteins prohibitins seemed to be affected in different ways by the two treatments. The Shotgun analysis revealed an upregulation of prohibitin after both treatments, whereas prohibitin 2 was raised only by MPP^+ treatment, probably as an effect of ATP depletion following complex I inhibition.[39] On the other hand, a 25 kDa prohibitin fragment identified by 2-DE displayed discordant changes after dopamine and MPP^+ treatment. This observation might reflect a different post-translational processing at the mitochondrial level that could lead to an alteration of mitochondria function and dynamics. Eventually, prohibitins regulate the activity of mAAA, a key participant in the quality control of inner membrane proteins.[36] This protease, together with the inner membrane protease PARL, regulates the PINK1-induced mitochondrial recruitment of parkin, a fundamental step in the quality control of mitochondria.[40]

A comprehensive pathway analysis of all proteins affected by dopamine allowed a deeper insight of the mechanisms that might be perturbed by altered dopamine homeostasis. Interestingly, the Parkinson's disease pathway and the Parkin–Ubiquitin Proteasomal System pathway were significantly over-represented, together with GO terms related to the generation of precursor metabolites and energy, the response to topologically incorrect proteins and the programmed cell death. Indeed, dopamine induced apoptosis in this cellular model, as expected,[19,30] together with alterations of the energetic metabolism. As far as quality control pathways are concerned, several members of the HSP70 chaperone family (*e.g.* mortalin, Heat shock 70 kDa protein 1A/1B) were observed to be affected by dopamine in the present study. HSP70 pathway seems to be functionally linked to the parkin–ubiquitin proteasomal system. First, parkin has been shown to mono-ubiquitinate HSP70 at several sites.[41] Moreover, it has been reported that the C-terminus HSP70-interacting protein (CHIP), HSP70 and parkin form a ternary complex that promotes ubiquitination and degradation of the Pael receptor, a protein whose accumulation has been linked to dopaminergic neuronal death.[42] Eventually, HSP70 levels are upregulated in the brain of sporadic PD cases and in parkin null mice but not in patients with early onset PD.[41,43,44]

The disease association analysis highlighted the significant classification of proteins as linked to mitochondrial disease. Interestingly, proteins in this list included ATP carriers, such as VDAC1 and ADP/ATP translocases, and components of the mitochondrial protein synthesis machinery, such as the mitochondrial ribosomal protein S22 and the elongation factor Tu. Together with the heat shock proteins discussed above, the upregulation of these proteins may activate compensatory mechanisms that eventually lead to apoptosis. Interestingly, the ADP/ATP translocase 3 can take part to the formation of the

mitochondrial permeability transition pore together with VDAC1.[45]

In conclusion, altered dopamine homeostasis induced several changes in the mitochondrial proteome that in part are due to a direct effect of dopamine on mitochondria (*e.g.*, alteration of the mitochondrial protease activity) and in part reflect the activation of processes that involve the mitochondria in a general response to dopamine (*e.g.*, regulation of programmed cell death). In particular, several pieces of evidence support the view that dopamine specifically activated mitochondrial proteases. The complete cleavage of VDAC2 into fragments that are still quantified by Shotgun is a clear-cut example of the dopamine-induced activation of proteolytic enzymes within mitochondria, further supported by mortalin and prohibitin fragmentation. Remarkably, the specific identification of proteolytic fragments and their comparison with the total amount of the original protein was only possible by integrating gel-based and gel-free approaches.

Experimental

Materials

Human neuroblastoma SH-SY5Y cells were obtained from the European Collection of Cell Cultures (Cat No. 94030304; Lot No. 11C016) and were cultured in 5% CO_2 humidified atmosphere at 37 °C in high-glucose Dulbecco's modified Eagle's medium (DMEM) with 10% fetal bovine serum (FBS), 100 U ml^{-1} penicillin, 100 μg ml^{-1} streptomycin, and 2 mM L-glutamine. Dopamine, catalase and MPP^+ were from Sigma Aldrich. All cell culture media and other reagents were from Euroclone.

Cytotoxicity assays

Cell viability was investigated using the neutral red (NR) uptake assay.[46] Cells were seeded in 24-well plates at 10^5 cells per well and cultured for 24 h at 37 °C before assay. The cells were exposed to different dopamine concentrations (0, 250 and 500 μM) and different MPP^+ concentrations (0, 1, 2.5, 3.5 and 5 mM) for 24 h. Catalase (700 U mL^{-1}) was added in each well to eliminate aspecific effects due to H_2O_2 arising from dopamine auto-oxidation.[19] At the end of the treatment, the conditioned medium was removed and cells were incubated with freshly prepared NR solution (50 μg ml^{-1} NR in culture medium) for 3 h at 37 °C. Then cells were rapidly washed with a fixative (1% $CaCl_2$ and 1.3% formaldehyde) and subsequently lysed with extraction solution (50% ethanol and 1% acetic acid). After 30 min incubation at RT, aliquots of the resulting solutions were transferred to cuvettes and the absorbance was recorded at 540 nm by using UV-Vis Optizen Pop 810 Nano Bio spectrophotometer (Mecasys). Results were expressed as a percentage of control. All experiments were run in triplicate. Statistical significance was assessed by the Welch-corrected *t* test.

Mitochondrial enriched fractions

Cells were cultured for 24 h in the absence and in the presence of 250 μM dopamine or 2.5 mM MPP^+, in the presence of 700 U ml^{-1} catalase. All experiments were run in five replicates for each condition. Cells were detached with Trypsin-EDTA and collected by centrifugation (300 × *g*, 25 °C, 7 min). Pellets were resuspended with the isolation buffer (250 mM sucrose, 10 mM Tris/MOPS pH 7.4, 1 mM EGTA, 10% v/v protease inhibitor mix) and mechanically disrupted by 30 strokes of a glass/glass Dounce homogenizer (in an ice bath).[32] Homogenates were centrifuged to eliminate cell debris (600 × *g*, 4 °C, 10 min) and supernatants were centrifuged again to isolate mitochondrial enriched fractions (10 000 × *g*, 4 °C, 10 min). The resulting pellets were washed in isolation buffer (2×) and stored in liquid nitrogen for further investigations. The efficiency of the isolation procedure was tested by western blotting quantification of histone H3 (nuclear marker, Upstate 07352, 1 : 3000), voltage-dependent anion channel VDAC1 (mitochondrial marker, Abcam ab15895, 1 : 600) and β-actin (cytoplasmic marker, GeneTex GTX23280, 1 : 3000).

Shotgun proteomics

Mitochondrial fractions were lysed in 50 μl of 0.1% RapiGest SF Surfactant (Waters, Milford, MA, http://www.waters.com) diluted in 50 mM $(NH_4)_2CO_3$, pH 8.0, according to the manufacturer's instructions, and the protein amount was determined using the Bradford method using the Bio-Rad Protein Assay Dye Reagent Concentrate (Bio-Rad). Tryptic digestion was performed in RapiGest SF as previously described.[47] Prior to proteolysis, mitochondrial fractions were subjected to reduction with 10 mM TCEP (30 min at 55 °C) and alkylation with 20 mM iodoacetamide (IAA; 30 min. at RT). Peptide digestion was conducted using 1.5 μg sequence-grade trypsin (Promega, Madison, WI, USA) at 37 °C overnight. The reaction was stopped by acidification with 0.1% formic acid (FA) at 37 °C for 30 minutes. To get rid of the acid-labile surfactant RapiGest SF, sample was centrifuged for 10 min at 16 200 × *g* and the supernatant saved for the LC MS^E analysis.

Samples were diluted with an aqueous solution of 0.1% FA, 3% CH_3CN (at a final peptide concentration of 0.4 μg μl^{-1}) and loaded onto a 5 μm Symmetry C18 trapping column 180 μm × 20 mm (Waters) and separated by a 170 min reversed phase gradient at 250 nL min^{-1} (3–40% CH_3CN over 145 min) on a nano ACQUITY UPLC System (Waters), using a 1.7 μm BEH 130 C18 Nano Ease 75 μm × 25 cm nano-scale LC column (Waters). 150 fmol μl^{-1} of MassPrepYeast Enolase digestion standard (Waters), prepared by digesting Yeast Enolase (UniProtKB/Swiss-Prot AC: P00924) with sequencing grade trypsin, were added to each sample as the internal standard. The lock mass ([Glu1]-Fibrinopeptide B, Sigma, 500 fmol μl^{-1}) was delivered from the auxiliary pump of the instrument with a constant flow rate of 600 nL min^{-1}. Separated peptides were mass analyzed by a hybrid quadrupole orthogonal acceleration time-of-flight mass spectrometer (Q-Tof Premier, Waters) directly coupled to the chromatographic system and programmed to step between low (4 eV) and high (15–40 eV) collision energies on the gas cell, using a scan time of 1.5 s per function over 50–1990 *m*/*z*.

Mass spectrometry data were acquired in Expression mode (MS^E), a data-independent parallel parent and fragment ion analysis without the selection of a fixed ion transmission

window on the first mass analyzer prior to collision induced dissociation.[48] Continuum LC-MS data from four replicates experiments for each samples were processed for qualitative and quantitative analysis using the software ProteinLynx Global Server v. 2.4 (PLGS, Waters Corp.).

Qualitative identification of proteins was obtained using the embedded ion accounting algorithm of the software PLGS 2.4 (Waters Corp.), searching in the human database UniProt KB/Swiss-Prot Protein Knowledgebase (release 2013_08, 24-July-13; 540732 sequence entries, comprising 192091492 amino acids abstracted from 221115 references; taxonomical restrictions: Human, 20266 sequences) to which data from *S. cerevisiae* Enolase were appended (UniProtKB/Swiss-Prot AC: P00924).[25,49] The search parameters included: automatic tolerance for precursor ions and for product ions, minimum of 3 fragment ions matched per peptide, minimum of 7 fragment ions matched per protein, minimum of 2 peptides matched per protein, 1 missed cleavage, carbamidomethylation of cysteine as fixed modification and oxidation of methionine as variable modification, false positive rate (FPR) fixed below 4% for protein identification and 150 fmol of the Yeast Enolase internal standard set as calibration protein concentration.[48]

The label free differential expression analysis was performed considering the 12 technical replicates available for each experimental condition (*i.e.*, one experimental condition × three biological replicates × four technical replicates) following the hypothesis that each treatment (DA, MPP^+ and control) is an independent variable. Within the differential analysis, EMRT clusters tables (*i.e.*, the list of peptide Exact Masses paired to their Retention Times) and Protein tables were generated upon normalization with the endogenous protein Human ATP synthase subunit β mitochondrial (ATP 5B, UniProtKB/Swiss-Prot AC: P06576). ATP 5B was chosen since, in the qualitative analysis, it was observed being identified within the first 15 most abundant protein (*i.e.*, with a high PLGS score) in all the 36 replicates analyzed (12 control, 12 DA and 12 MPP^+).

The most reproducible proteotypic peptides of ATP 5B for retention time and intensity (*m*/*z* 975.56, *m*/*z* 1038.59, *m*/*z* 1088.65, *m*/*z* 1435.75 and *m*/*z* 1988.035) were used to normalize the EMRT table. Quantitative analysis was performed based on 164086 molecular spectral features using the EMRT cluster annotation. The differentially expressed proteins dataset was filtered by considering only those identifications from the alternate scanning LC-MS^E data exhibiting a good replication rate (at least 8 out of 12 injections, 66%) and with $p < 0.05$ for the relative protein fold change (two-tailed Student's *t* test). The significance of regulation level specified at ±30%, hence 1.3-fold (±0.26 on a natural log scale), which is typically 2–3 times higher than the estimated error on the intensity measurement, was used as a threshold to identify significant up- or down-regulation.[48]

Off-line statistical analysis of shotgun proteomics data

As an alternative evaluation of statistical significance, protein amounts obtained by the qualitative identification described above (see ''Shotgun proteomics'' paragraph of this section) were analyzed by modifying a procedure developed for the analysis of 2-DE image quantifications.[2,4,50,51] Protein amounts were imported together with UniProtKB/Swiss-Prot AC and descriptions for each of the 36 LC-MS/MS experiments (four technical replicates, three independent experiments, three experimental conditions each). This procedure allowed identifying 537 proteins. A table was built for each UniProtKB/Swiss-Prot AC and subsequently filtered to eliminate all proteins that displayed two or more missed quantifications in all four technical replicates (*e.g.*, all replicates of the same sample failed to quantify the protein). The filtered dataset was then reduced to 80 proteins. Each protein amount was normalized with respect to the amount of ATP 5B, transformed into a $\log_2$ scale for comparative statistics using parametric tests[55] and scaled to the median value of the control group. Semi-quantitative differences were evaluated by paired *t* test between each treatment (*i.e.*, DA or MPP^+) and the control condition. In order to avoid type-II (beta) errors in the subsequent bioinformatics analysis, no correction for multiple testing was applied. All procedures for data analysis and graphics were written in ***R***, an open-source environment for statistical computing.[52]

Two-dimensional electrophoresis and statistical analysis

Mitochondria were suspended in 100 μl lysis solution (7 M, urea, 2 M thiourea, 4.8 mM tris(2-carboxyethyl)phosphine hydrochloride (TCEP-HCl), 4% w/v 3-[(3-cholamidopropyl)dimethylammonio]-1-propanesulfonate (CHAPS), 2% w/v amidosulfobetaine-14 (ASB-14), 1% v/v IPG buffer 3–10 nonlinear (GE Healthcare), 0.5 μl protease inhibitor mix).[31] After 1 h extraction at RT, mitochondria were lysed by sonication (10 × 0.2 s) and centrifuged (20 000 × *g*, 20 °C, 40 min) to precipitate organelle debris. In order to remove nucleic acids and lipids that could interfere with 2-DE, 100 μl mitochondrial protein solution were diluted twenty-fold in UTC (7 M urea, 2 M thiourea and 4% CHAPS). Each sample was transferred into an ultrafiltration concentration device (Vivaspin 500 MWCO 3000 Da PES, Sartorius) and centrifuged at 15 000 × *g* to a final 100 μl volume. Protein concentration in the supernatant was determined using the Bio-Rad Protein Assay (Bio-Rad). Total proteins (200 μg) were diluted to 260 μl with a buffer containing 7 M urea, 2 M thiourea, 4.8 mM TCEP-HCl, 4% CHAPS, 2% w/v ASB-14, 1% IPG buffer 3–10 NL, and traces of bromophenol blue, and loaded onto 13 cm IPG DryStrips (GE Healthcare, Little Chalfont, UK) with a non-linear 3–10 pH gradient by in-gel rehydration (1 h at 0 V, 10 h at 50 V). IEF was performed at 20 °C on IPGphor (GE Healthcare) according to the following schedule: 2 h at 200 V, 2 h linear gradient to 2000 V, 2 h at 2000 V, 1 h of linear gradient to 5000 V, 2 h at 5000 V, 2 h linear gradient to 8000 V and 3 h and 30 min at 8000 V. IPG strips were then equilibrated for 2 × 30 min in 50 mM Tris-HCl pH 8.8, 6 M urea, 30% glycerol, 2% SDS and traces of bromophenol blue containing 5 mM TCEP-HCl for the first equilibration step and 2.5% iodoacetamide for the second one. SDS-PAGE was performed using 13% 1.5 mm thick separating polyacrylamide gels without stacking gel, using a Hoefer SE 600 system (GE Healthcare). The second dimension was carried out at 45 mA per gel, 18 °C. Molecular weight marker proteins (10–200 kDa from Fermentas, Burlington, Canada) were used for calibration.

The resulting maps were stained with Ru(II) tris(bathophenanthroline disulfonate) (Serva). Images were acquired (12 bit grayscale) with the GelDoc-It Imaging System (UVP) and analyzed with ImageMaster 2D Platinum (GE Healthcare). Spots were detected automatically by the software and manually refined hereafter; gels were then matched and the resulting clusters of spots confirmed manually. Unmatched spots among the experimental groups were considered as qualitative differences. Spots have been quantified on the basis of their relative volume (spot volume normalized to the sum of the volumes of the common spots).[50,51] Gel reproducibility was assessed by Q–Q plots.[51,52] Missing values were replaced by the minimum value observed for that spot (if the mean spot volume was in the lower 5th percentile) or to the mean value observed in the group.[53] Quantitative differences were assessed by the non-parametric Kruskal–Wallis analysis of variance followed by *post hoc* Dunn's test.[54] In order to avoid type-II (beta) errors in the subsequent bioinformatics analysis, no correction for multiple testing was applied. All procedures for data analysis and graphics were written in ***R***, an open-source environment for statistical computing.[55]

Protein excision and tryptic digestion

Protein spots were excised manually and transferred into Eppendorf tubes (0.2 ml), washed with water and gradually dehydrated by subsequent passages in 50 mM NH_4HCO_3, 50% CH_3CN in 50 mM NH_4HCO_3 and 100% CH_3CN. Gel-immobilized proteins were reduced with 10 mM DTT, alkylated with 55 mM IAA, washed with 50 mM NH_4HCO_3 and dehydrated in CH_3CN as described above until completely dry. Dry spots were reswollen with a solution of 10 ng μl^{-1} trypsin in 50 mM NH_4HCO_3 and digested overnight at 37 °C. Upon digestion, peptides obtained from each spot were gel extracted by subsequent washes with 1% TFA and 60% CH_3CN in 0.1% TFA and collected in a fresh tube, vacuum dried and resuspended in 20 μl 3% CH_3CN, 0.1% TFA solution for further analysis by ESI-TRAP LC-MS.

LC-MS analysis in ESI-TRAP

Tryptic digests were analyzed by nLC-MS on a Proxeon EASY-nLCII (Thermo Fisher Scientific, Milan, Italy) interfaced with an amaZon ETD Ion Trap (Bruker Daltonics). Volumes of 15 μl from each sample were injected and pre-concentrated for 3 min on a C18-A1 EASY-Column™ (2 cm, 100 μm I.D., 5 μm p.s., Thermo Fisher Scientific) at a flow rate of 5 $\mu l\ min^{-1}$. A gradient elution was performed on a C18-Acclaim PepMap (25 cm, 75 μm I.D., 5 μm p.s., Thermo Fisher Scientific), flow rate: 0.3 $\mu l\ min^{-1}$, T 20 °C; eluents: A, 0.1% HCOOH in H_2O and B, 0.1% HCOOH in CH_3CN; gradient: from 3 to 30% B in 60 min. MS data were acquired using an AutoMSn method (Bruker Daltonics definition for data dependent acquisition) using the enhanced resolution as scan mode (15 000 $m/z\ s^{-1}$). Ten precursor ions were selected for each survey scan, keeping the active exclusion enabled for 30 seconds after 2 MS^2 scans on the same precursor. Raw data were processed using the Bruker DATA Analysis (HappyChunks_mgfgeneration_02-11.m) to generate a peak list for database searching. Protein IDs were performed using the MASCOT v.2.4.1 algorithm (http://www.matrixscience.com), against Uniprot/Swiss-Prot non-redundant database version 2013-08 restricted to *Homo sapiens* taxonomy (20266 sequences), setting carbamidomethylation of cysteines as fixed modification and oxidation of methionines as variable modification, allowing one missing cleavage. A maximal error tolerance of 0.4 Da and 0.5 Da was chosen for parent and fragment ions, respectively, according to the low resolution mass analyzer. Mascot protein scores >33 were considered significant ($p < 0.05$) for protein identification assignment.

Bioinformatics

Proteins identified by shotgun proteomics were classified for cellular compartment ontology using DAVID functional annotation tools (http://david.abcc.ncifcrf.gov/). The list of 80 refined proteins (see Paragraph *Off-line statistical analysis of shotgun proteomics data*) was fed to the search engine for classification with the proprietary GOTERM_CC_FAT dataset.

The list of all identified proteins was fed to BioProfiling (http://www.bioprofiling.de/) to obtain the network enrichment, based on known physical protein–protein interactions (IntAct Database). The significant analyses, $p < 0.01$, were further considered to interpret and discuss proteomics results. The estimate of the *p*-value provided by the Monte Carlo procedure corresponds to the probability to get a model of the same quality for a random gene list of the same size (random networks statistical environment).[56] Eventually, the enriched network was exported as a .xgmml file and visualized and modified using Cytoscape (http://www.cytoscape.org/). The Gene Ontology, the KEGG pathway, the Wikipathway and the disease association enrichment analyses were carried out using the Webgestalt online tools (http://bioinfo.vanderbilt.edu/webgestalt/). Hereby, the entire human genome was used as a reference set. Fisher's exact test with Benjamini & Hochberg adjustment for multiple comparisons was employed to control the threshold of statistical overrepresentation of biochemical pathways. The 10 pathways with the most significant *p* values were considered.[57]

Dataset deposition

The mass spectrometry proteomics data have been deposited to the ProteomeXchange Consortium (http://proteomecentral.proteomexchange.org) *via* the PRIDE partner repository[58] with the dataset identifier PXD000838.

Acknowledgements

We thank Dr Gabriella Fanali for helpful discussion. We thank Tobias Ternent and the PRIDE Team for the processing and deposition of our mass spectrometry data into the ProteomeXchange database. This work was supported by the Italian Ministry of Education and University (PRIN grant no. 2009CCZSES to M.F.). This study is part of the Italian HPP initiative dedicated to mitochondria coordinated by A.U.

References

1 J. M. Shulman, P. L. De Jager and M. B. Feany, *Annu. Rev. Pathol.: Mech. Dis.*, 2011, **6**, 193–222.
2 T. Alberio, L. Lopiano and M. Fasano, *FEBS J.*, 2012, **279**, 1146–1155.
3 F. Blandini and M. T. Armentero, *FEBS J.*, 2012, **279**, 1156–1166.
4 T. Alberio and M. Fasano, *J. Biotechnol.*, 2011, **156**, 325–337.
5 M. Bisaglia, E. Greggio, M. Beltramini and L. Bubacco, *FASEB J.*, 2013, **27**, 2101–2110.
6 A. M. Cuervo, E. S. Wong and M. Martinez-Vicente, *Mov. Disord.*, 2010, **25**(suppl 1), S49–S54.
7 M. Xilouri and L. Stefanis, *Expert Rev. Mol. Med.*, 2011, **13**, e8.
8 A. Puschmann, *Parkinsonism Relat. Disord.*, 2013, **19**, 407–415.
9 N. Exner, A. K. Lutz, C. Haass and K. F. Winklhofer, *EMBO J.*, 2012, **31**, 3038–3062.
10 S. Lehmann and L. M. Martins, *J. Mol. Med.*, 2013, **91**, 665–671.
11 C. Perier and M. Vila, *Cold Spring Harbor Perspect. Med.*, 2012, **2**, a009332.
12 L. H. Sanders and J. T. Greenamyre, *Free Radical Biol. Med.*, 2013, **62**, 111–120.
13 E. S. Vincow, G. Merrihew, R. E. Thomas, N. J. Shulman, R. P. Beyer, M. J. MacCoss and L. J. Pallanck, *Proc. Natl. Acad. Sci. U. S. A.*, 2013, **110**, 6400–6405.
14 M. R. Duchen, *Pfluegers Arch.*, 2012, **464**, 111–121.
15 D. A. Kubli, M. N. Quinsay and A. B. Gustafsson, *Commun. Integr. Biol.*, 2013, **6**, e24511.
16 D. Narendra, A. Tanaka, D. F. Suen and R. J. Youle, *J. Cell Biol.*, 2008, **183**, 795–803.
17 D. Narendra, L. A. Kane, D. N. Hauser, I. M. Fearnley and R. J. Youle, *Autophagy*, 2010, **6**, 1090–1106.
18 S. Geisler, K. M. Holmström, D. Skujat, F. C. Fiesel, O. C. Rothfuss, P. J. Kahle and W. Springer, *Nat. Cell Biol.*, 2010, **12**, 119–131.
19 T. Alberio, A. M. Bossi, A. Milli, E. Parma, M. B. Gariboldi, G. Tosi, L. Lopiano and M. Fasano, *FEBS J.*, 2010, **277**, 4909–4919.
20 G. Marko-Varga, G. S. Omenn, Y. K. Paik and W. S. Hancock, *J. Proteome Res.*, 2013, **12**, 1–5.
21 A. Urbani, M. De Canio, F. Palmieri, S. Sechi, L. Bini, M. Castagnola, M. Fasano, A. Modesti, P. Roncada, A. M. Timperio, L. Bonizzi, M. Brunori, F. Cutruzzolà, V. De Pinto, C. Di Ilio, G. Federici, F. Folli, S. Foti, C. Gelfi, D. Lauro, A. Lucacchini, F. Magni, I. Messana, P. P. Pandolfi, S. Papa, P. Pucci, P. Sacchetta and Italian Mt-Hpp Study Group-Italian Proteomics Association (www.itpa.it), *Mol. Biosyst.*, 2013, **9**, 1985–1992.
22 B. Leroy, N. Houyoux, S. Matallana-Surget and R. Wattiez, in *Integrative Proteomics*, ed. H.-C. Leung, INTECH, 2012, pp. 327–346.
23 V. Gautier, E. Mouton-Barbosa, D. Bouyssié, N. Delcourt, M. Beau, J. P. Girard, C. Cayrol, O. Burlet-Schiltz, B. Monsarrat and A. Gonzalez de Peredo, *Mol. Cell. Proteomics*, 2012, **11**, 527–539.
24 V. Marzano, S. Santini, C. Rossi, M. Zucchelli, A. D'Alessandro, C. Marchetti, M. Mingardi, V. Stagni, D. Barilà and A. Urbani, *J. Proteomics*, 2012, **75**, 4632–4646.
25 L. Pieroni, F. Finamore, M. Ronci, D. Mattoscio, V. Marzano, S. L. Mortera, S. Quattrucci, G. Federici, M. Romano and A. Urbani, *Mol. Biosyst.*, 2011, **7**, 630–639.
26 C. Vogel and E. M. Marcotte, *Methods Mol. Biol.*, 2012, **893**, 321–341.
27 D. Xu, S. Suenaga, M. J. Edelmann, R. Fridman, R. J. Muschel and B. M. Kessler, *Mol. Cell. Proteomics*, 2008, **7**, 2215–2228.
28 D. N. Hauser and T. G. Hastings, *Neurobiol. Dis.*, 2013, **51**, 35–42.
29 F. M Lopes, R. Schröder, M. L. da Frota Jr, A. Zanotto-Filho, C. B. Müller, A. S. Pires, R. T. Meurer, G. D. Colpo, D. P. Gelain, F. Kapczinski, J. C. Moreira, C. Fernandes Mda and F. Klamt, *Brain Res.*, 2010, **1337**, 85–94.
30 C. Gómez-Santos, I. Ferrer, A. F. Santidrián, M. Barrachina, J. Gil and S. Ambrosio, *J. Neurosci. Res.*, 2003, **73**, 341–350.
31 T. Rabilloud, *Methods Mol. Biol.*, 2008, **432**, 83–100.
32 C. Frezza, S. Cipolat and L. Scorrano, *Nat. Protocols*, 2007, **2**, 287–295.
33 L. Ting, M. J. Cowley, S. L. Hoon, M. Guilhaus, M. J. Raftery and R. Cavicchioli, *Mol. Cell. Proteomics*, 2009, **8**, 2227–2242.
34 A. Rogowska-Wrzesinska, M. C. Le Bihan, M. Thaysen-Andersen and P. Roepstorff, *J. Proteomics*, 2013, **88**, 4–13.
35 A. H. Schapira, *Exp. Neurol.*, 2010, **224**, 331–335.
36 P. Martinelli and E. I. Rugarli, *Biochim. Biophys. Acta*, 2010, **1797**, 1–10.
37 R. Shanbhag, G. Shi, J. Rujiviphat and G. A. McQuibban, *Parkinson's Dis.*, 2012, 382175.
38 J. Jin, C. Hulette, Y. Wang, T. Zhang, C. Pan, R. Wadhwa and J. Zhang, *Mol. Cell. Proteomics*, 2006, **5**, 1193–1204.
39 M. Artal-Sanz and N. Tavernarakis, *Trends Endocrinol. Metab.*, 2009, **20**, 394–401.
40 A. W. Greene, K. Grenier, M. A. Aguileta, S. Muise, R. Farazifard, M. E. Haque, H. M. McBride, D. S. Park and E. Fon, *EMBO Rep.*, 2012, **13**, 378–385.
41 D. J. Moore, A. B. West, D. A. Dikeman, V. L. Dawson and T. M. Dawson, *J. Neurochem.*, 2008, **105**, 1806–1819.
42 Y. Imai, M. Soda, S. Hatakeyama, T. Akagi, T. Hashikawa, K. I. Nakayama and R. Takahashi, *Mol. Cell*, 2002, **10**, 55–67.
43 J. A. Rodríguez-Navarro, M. J. Casarejos, J. Menéndez, R. M. Solano, I. Rodal, A. Gómez, J. G. Yébenes and M. A. Mena, *J. Neurochem.*, 2007, **103**, 98–114.
44 K. Gaweda-Walerych and C. Zekanowski, *Acta Neurobiol. Exp.*, 2013, **73**, 199–224.
45 C. Pereira, N. Camougrand, S. Manon, M. J. Sousa and M. Côrte-Real, *Mol. Microbiol.*, 2007, **66**, 571–582.
46 G. Repetto, A. del Peso and J. L. Zurita, *Nat. Protoc.*, 2008, **3**, 1125–1131.
47 F. Mbeunkui and M. B. Goshe, *Proteomics*, 2011, **11**, 898–911.
48 J. P. Vissers, J. I. Langridge and J. M. Aerts, *Mol. Cell. Proteomics*, 2007, **6**, 755–766.
49 J. C. Silva, R. Denny, C. A. Dorschel, M. Gorenstein, I. J. Kass, G. Z. Li, T. McKenna, M. J. Nold, K. Richardson,

P. Young and S. Geromanos, *Anal. Chem.*, 2005, **77**, 2187–2200.
50 T. Alberio, A. C. Pippione, M. Zibetti, S. Olgiati, D. Cecconi, C. Comi, L. Lopiano and M. Fasano, *Sci. Rep.*, 2012, **2**, 953.
51 M. Fasano and T. Alberio, *Protocol Exchange*, 2013, DOI: 10.1038/protex.2013.001.
52 T. Alberio, E. M. Bucci, M. Natale, D. Bonino, M. Di Giovanni, E. Bottacchi and M. Fasano, *J. Proteomics*, 2013, **90**, 107–114.
53 D. Albrecht, O. Kniemeyer, A. A. Brakhage and R. Guthke, *Proteomics*, 2010, **10**, 1202–1211.
54 J. H. McDonald, *Handbook of Biological Statistics*, Sparky House Publishing, Baltimore, 2nd edn, 2009.
55 R Development Core Team, *R: A language and environment for statistical computing*, R Foundation for Statistical Computing, Vienna, 2009.
56 A. V. Antonov, S. Dietmann, I. Rodchenkov and H. W. Mewes, *Proteomics*, 2009, **9**, 2740–2749.
57 B. Zhang, S. Kirov and J. Snoddy, *Nucleic Acids Res.*, 2005, **33**, W741–W748.
58 J. A. Vizcaino, R. G. Cote, A. Csordas, J. A. Dianes, A. Fabregat, J. M. Foster, J. Griss, E. Alpi, M. Birim, J. Contell, G. O'Kelly, A. Schoenegger, D. Ovelleiro, Y. Perez-Riverol, F. Reisinger, D. Rios, R. Wang and H. Hermjakob, *Nucleic Acids Res.*, 2013, **41**, D1063–D1069.

